Effects of the Intramolecular Disulfide Bond on Ligand Binding Dynamics in Myoglobin†

Takeshi Uchida, Masashi Unno,‡ Koichiro Ishimori, and Isao Morishima*

Department of Molecular Engineering, Graduate School of Engineering, Kyoto University, Kyoto 606-01, Japan

Received March 11, 1996; Revised Manuscript Received August 12, 1996⊗

ABSTRACT: In order to investigate the effects of an intramolecular disulfide bond on protein structure and ligand binding dynamics in myoglobin, we prepared a mutant myoglobin having a disulfide bond at the EF corner by introducing two cysteine at the position of Ile 75 and Glu 85. On the basis of the spectral features of the mutant, the formation of the disulfide bond only affected minor structural deviations of the heme environmental structure in the carbonmonoxy form, whereas more substantial structural alterations were induced in the deoxygenated form. Laser photolysis experiments for carbon monoxide rebinding clearly showed that the artificial S−S bond accelerates the bimolecular rebinding rate from 1.0 to 1.8 μM^{-1} s^{-1} and increases the geminate yield from 0.072 to 0.092. The ligand migration rate from the solvent to the heme pocket and the bond formation rate from the heme pocket to the heme iron also increased. The free energy diagram for the mutants indicates that the energy barrier for the bond formation was raised as well as that for the ligand migration by introduction of the disulfide bond. However, the effects of the disulfide linkage at the EF corner on the kinetic parameter is much smaller than those of the amino acid substitutions located in the heme cavity. We can conclude that the perturbation of the protein fluctuations by formation of the disulfide bond would be localized at the mutation site or the contributions from other regions and motions might be more important for the ligand binding dynamics.

The protein fluctuation plays key roles not only in the protein folding but also in the substrate binding dynamics for many enzymes (Gurd & Rothgeb, 1979; Karplus & McCammon, 1983). X-ray structures of hemoproteins have shown that there are no ligand entry channels even for small molecules such as the oxygen molecule or carbon monoxide (Takano, 1977; Phillips, 1980). This observation implies that the ligand binding process requires protein structural fluctuations. Although a number of the kinetic experiments over wide ranges of time and temperature have enabled us to investigate the effects of the protein fluctuation on the ligand binding dynamics of hemoproteins, molecular mechanisms for regulation of the ligand binding by the protein fluctuation are still unclear (Gibson et al., 1986; Austin et al., 1975; Henry et al., 1983; Olson et al., 1988; Frauenfelder et al., 1991; Steinback et al., 1991; Lambright et al., 1991; Tian et al., 1996).

To elucidate the effect of protein fluctuation on ligand binding, we introduced an artificial disulfide bond into myoglobin (Mb), which is a globular protein of about molecular weight 18 000 and 153 amino acid residues and contains one protoheme. Intensive studies on the ligand binding kinetics of myoglobin (Springer et al., 1994, and references therein) have revealed the detailed mechanism of the ligand binding process on the time scale from picosecond to second, which led myoglobin to be one of the most basic and conventional model systems to examine dynamic properties of proteins. However, most of the previous studies have focused on the regulation mechanism by single or some amino acid residues around the distal or proximal histidine, and little attention has been paid to the protein fluctuation including global motion of helices of myoglobin in the ligand binding.

The disulfide bond, which is formed by the oxidation of a pair of cysteines, has been considered to be one of the major structural factors for the protein fluctuation (Kidera et al., 1992; Careaga & Falke, 1992; Daggett & Levitt, 1993; Jeng & Dyson, 1995). Previous studies have shown that introduction of artificial disulfide bonds into a protein molecule enhanced protein stability by lowering the entropy of the unfolding state and enthalpic stabilization of the folded state (Perry & Wetzel, 1984; Pantoliano et al., 1987; Matsumura et al., 1989; Kanaya et al., 1991; Gusev et al., 1991), indicating that a disulfide bond perturbs or restricts the protein fluctuations. Since the protein fluctuation should be essential to protein function as well as to stabilize protein structure, introduction of disulfide bonds would be critical for the ligand binding dynamics in myoglobin.

On the basis of the temperature-dependent X-ray diffraction, Frauenfelder et al. (1979) pointed out large mean-square displacement in the EF corner, F-helix, and GH corner upon the ligand binding. These regions are close to the heme and might be involved in a dynamic control mechanism in myoglobin and hemoglobin as suggested by Perutz (1965). Of these regions showing the large *B*-factor, we focused on the E- and F-helices, in which the proximal and distal histidines are located. As shown in the crystal structure (Takano, 1977; Phillips, 1980), the proximal histidine is the only amino acid residue coordinating to the heme iron and the distal histidine directly interacts with the bound oxygen

† This work was supported by Grants 07309006 and 07558215 (to I.M.) for scientific research and Research Grant 06808058 (to K.I.) from the Ministry of Education, Science, Culture, and Sports.

* To whom correspondence should be addressed. Fax: +81-75-751-7611. Phone: +81-75-753-5921. E-mail: morisima@mds.moleng.kyoto-u.ac.jp.

‡ Present address: Department of Physics, Northeastern University, Boston, MA 02115.

⊗ Abstract published in *Advance ACS Abstracts,* December 15, 1996.

S0006-2960(96)00591-0 CCC: $14.00

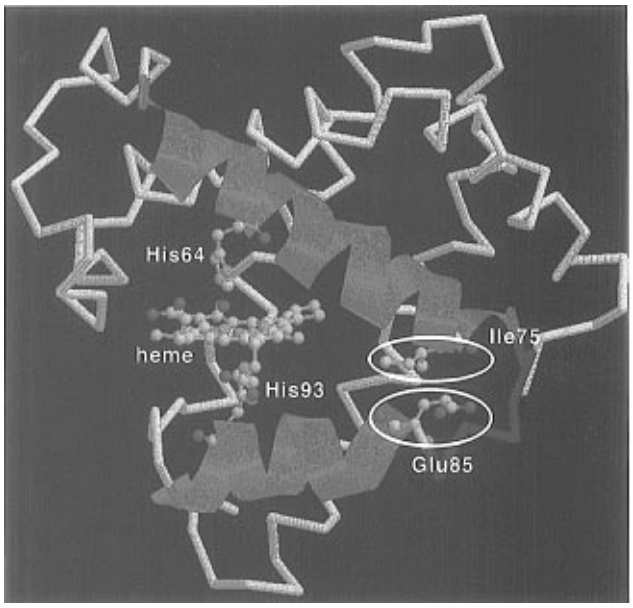

FIGURE 1: Introduction site of the disulfide bond in human myoglobin. The mutated residues, Ile 75 and Glu 85, are circled. The E- and F-helices are described by the ribbon model, and the other part is described by the α-carbon backbone structure.

at the heme iron. Since the E- and F-helices would move away to let the oxygen molecule migrate from the solvent to the heme iron, restriction of the fluctuations of these two helices by formation of the disulfide bond would affect ligand binding properties of myoglobin and offer unique information for dynamics of the ligand binding.

In order to perturb the motion of the E- and F-helices, we mutated isoleucine-75 (Ile 75) and glutamic acid-85 (Glu 85) to cysteine to form a disulfide bond in the EF corner (Figure 1). Ile 75 is located at the end of the E-helix, and the position of Glu 85 is the beginning of the F-helix. The distance between the γ-methylene carbon of Ile 75 and the γ-carbonyl carbon of Glu 85 is about 4.05 Å in the carbonmonoxy form (Cheng & Schoenborn, 1991), which is not far from the length of a typical disulfide bond (2.0 Å) (Phillips, 1966), showing that Ile 75 and Glu 85 are one of the most appropriate amino acid pairs to form an intramolecule disulfide bond between E- and F-helices. We examined the effects of the intramolecular disulfide bond on the static structure of the liganded and unliganded forms by various spectroscopies and the carbon monoxide binding properties of the mutant myoglobin in the absence and presence of the disulfide bond by laser photolysis under various hydrostatic pressures.

MATERIALS AND METHODS

Reagents and Protein Preparation. Potassium ferricyanide, DTT,[1] and sodium dithionite were purchased from Wako Pure Chemical Industries, Ltd.

The original expression vector of human myoglobin, pMb3 (pLcIIFXMb), is a gift from Varadarajan and Boxer (Varadarajan et al., 1985). The procedures for site-directed mutagenesis are described in previous papers (Kunkel, 1985; Varadarajan et al., 1989; Adachi et al., 1992). DNA sequencing for the mutated myoglobin genes was performed by the DyeDeoxy Terminator method by using an ABI 373A DNA sequencer and was analyzed by a 373A DNA sequencing system. Protein preparation and purification were followed by the method described previously (Varadarajan et al., 1989; Adachi et al., 1992).

The spectroscopic and functional properties of the recombinant wild-type myoglobin[2] were indistinguishable from those of the native myoglobin (Varadarajan et al., 1989). The buffer solutions were 0.1 M sodium phosphate buffer, pH 7.0. The electronic absorption spectra of the deoxy, oxy, and carbonmonoxy forms of the mutants are similar to those of the wild-type protein. The peak maxima did not shift for more than 1 nm by the mutation.

Oxidation and Reduction of the Disulfide Bond. To form the intramolecular disulfide bond in the mutant, the purified protein was oxidized by 2 equiv of potassium ferricyanide ($K_3[Fe(CN)_6]$) at 37 °C for 12 h. An excess amount of ferricyanide was removed by a gel filtration column (Sephadex G-25) with 0.1 M sodium phosphate buffer at pH 7.0. By addition of a small amount of solid sodium dithionite, the heme iron was reduced to the ferrous state without cleavage of the disulfide bond. To cleave the disulfide bond, the purified protein was incubated with 100 mM DTT and 1 mM EDTA at 37 °C for 12 h under CO atmosphere.

Laser Photolysis Experiments. The methods for milli- and microsecond laser photolysis measurements are followed by the procedure previously reported (Adachi & Morishima, 1989; Adachi et al., 1992; Unno et al., 1994). A flashlamp-pumped dye laser with a half-peak duration of 300 ns (UNISOKU LA-501) was used. Rhodamine 6G (Kodak) in methanol was used to produce an excitation pulse at a wavelength maximum of 590 nm. The probe light at 436 nm was focused onto the slit of the monochromator (UNISOKU USP-501) and detected by a photomultiplier. A transient memory (GRAPHTEC TMR-80) was used to digitize the signal (50 ns/point, 4096 points), and data were transferred to a NEC PC-9801VX computer for further data analysis. The sample concentration was about 20 μM.

Ligand rebinding to the mutant and wild-type myoglobins was analyzed by fitting to the equation:

$$\Delta A_t = \Delta A_0 \exp(-k_{app}t) \quad (1)$$

where ΔA_t is the absorbance change at any time t and ΔA_0 is the total absorbance change (absorbance at $t = 0$ minus absorbance at $t = \infty$). k_{app} is the observed first-order rate constant, and the k_{app} satisfies the equation (Antonini & Brunori, 1971):

$$k_{app} = k_{on}[CO] \quad (2)$$

where k_{on} is the bimolecular ligand binding rate constant.

Over the narrow range of temperature (275−315 K) in these measurements, the overall rate constants showed a temperature dependence which obeys an Arrhenius law:

[1] Abbreviations: DTT, dithiothreitol; SDS−PAGE, sodium dodecyl sulfate−polyacrylamide gel electrophoresis; FT-IR, Fourier transform infrared; TMS, tetramethylsilane; ppm, parts per million; EDTA, ethylenediaminetetraacetate; WEFT, water-eliminated Fourier transform; FAB, fast atom bombardment.

[2] Varadarajan et al. (1989) replaced cysteine-110 of human myoglobin by alanine to prevent difficulties in protein purification. In this study, we denote this mutant (Cys 110 → Ala) of human myoglobin as "wild type".

$$k_{on} = A \exp(-E_a/RT) \quad (3)$$

where E_a is the activation energy and A is the prefactor (Chatfield et al., 1990).

For the nanosecond laser photolysis experiments, we used 6 ns FWHM pulses from a Q-switched Nd:YAG laser for the experiment. The incident energy was about 10 mJ. The absorption changes were monitored by a continuous, weak probe beam from a 150 W xenon arc lamp passed through a monochromator. The probe wavelength was 440 nm. Signals were detected in transmission using a photomultiplier (Hamamatsu Photonics, R2949), and the transient signals were digitized using an Iwatsu DS-8621 oscilloscope. Signals were averaged 150−240 times. The data were transferred to a NEC PC-9821Ae computer for further data analysis. No smoothing artifact affected the results of the following data analysis. The protein concentration was about 10 μM. The time courses were analyzed by fitting to the equation:

$$\Delta A_t/\Delta A_0 = \phi_g \exp(-k_g t) + (1 - \phi_g) \exp(-k_{on} t) \quad (4)$$

where k_g is the geminate rate constant, ϕ_g is the geminate yield, and ΔA_0 is the total absorbance change (absorbance at $t = 0$ minus absorbance at $t = \infty$).

In this study, we assumed the simple three-state sequential scheme (Henry et al., 1983):

$$\text{A (MbCO)} \underset{k_{BA}}{\overset{h\nu}{\rightleftharpoons}} \text{B (Mb}\cdots\text{CO)} \underset{k_{SB}}{\overset{k_{BS}}{\rightleftharpoons}} \text{S (Mb + CO)} \quad (5)$$

where the symbol A represents the liganded state in which CO is bounded to the heme iron (carbonmonoxy form) and S is unliganded form (deoxy form). B is a geminate state in which the iron−CO bond has been photolyzed but CO is still trapped within the protein (Henry et al., 1983; Lambright et al., 1989; Carver et al., 1990). The observable k_g (geminate rate constant), ϕ_g (geminate yield), and k_{on} (pseudo-first-order association rate constant) are related to the rate constants for the three-state sequential scheme (Lambright et al., 1989) by the equations:

$$k_g = k_{BA} + k_{BS} \quad (6)$$

$$\phi_g = k_{BA}/k_g = k_{BA}/(k_{BA} + k_{BS}) \quad (7)$$

$$k_{on} = k_{SB}\phi_g = k_{SB}k_{BA}/(k_{BA} + k_{BS}) \quad (8)$$

$$k_{off} = k_{AB}(1 - \phi_g) \quad (9)$$

Since we defined the activation energy as expressed by eq 3, it is presumed that the preexponential factor, A, of each step was equal to each other, which is adequate in our case (Carver et al., 1990). The absolute values of the preexponential factor do not affect the differences between the barrier height for the mutants (Carver et al., 1990).

Laser Photolysis Measurement under Various Pressures and Temperatures. The methods for milli- and microsecond laser photolysis measurements under various pressures have been described in our previous papers (Adachi & Morishima, 1889; Unno et al., 1990, 1991, 1994). All experiments under high pressure were performed in 0.1 M Tris-HCl buffer, pH 7.8. The pH of Tris buffer has been shown to be independent of pressure up to 200 MPa (Newmann et al., 1973). The activation volume is given by the equation:

$$\Delta V^{\ddagger} = -RT\left(\frac{\partial(\ln k_p/k_1)}{\partial P}\right)_T \quad (10)$$

where R is the gas constant (=8.314 J K^{-1} mol^{-1}), T is absolute temperature, and k_1 and k_p are observed first-order rate constants at 0.1 and P MPa, respectively. The slopes of the plot of ln k_p/k_1 versus pressure for the mutant myoglobins at atmospheric pressure were calculated by the optimized second-order polynomial function.

Dissociation Constant of Carbon Monoxide. The kinetic measurements of the CO dissociation rates were carried out with a UV−visible spectrometer (SHIMADZU UV-2200). k_{off} was determined by analyzing the replacement reaction in which ligated CO was replaced by NO as described in detail by Lambright et al. (1989). The concentrated myoglobin stocks were converted to the carbonmonoxy form by stirring under CO followed by reduction with sodium dithionite. NO-saturated buffer (100 mM sodium phosphate for pH 7.0) was prepared by bubbling NO through 3 mL of buffer in a sealed 1 cm path-length UV cell. About 20 μL of the concentrated MbCO solution was then injected into the cell at 20 °C, and the reaction was followed by monitoring the absorbance at 424 nm. The decay was fit to a single exponential using a nonlinear least-squares fitting.

The free energy change for the ligand binding in the deoxy and geminate states is calculated by the equations (Antonini & Brunori, 1971):

$$\Delta G = -RT \ln K_{CO} \quad (11)$$

$$\Delta\Delta G = -RT \ln\{K_{CO}(S-S)/K_{CO}(SH)\} \quad (12)$$

where K_{CO} is the equilibrium constant for CO binding (k_{on}/k_{off}).

FT-IR Spectra. The infrared spectra were measured at 1 cm^{-1} resolution on a Bio-Rad FTS-30 spectrophotometer. The sample concentration was about 1 mM. A small amount of sodium dithionite was added to remove residual oxygen just prior to recording the infrared spectra. Approximately 40 μL of carbonmonoxymyoglobin solution was loaded into a CaF_2 cell with 0.1 mm path length. We used an equimolar amount of wild-type aquometmyoglobin as a reference. Each spectrum was an average of 512 scans. To determine the peak positions and line width, we fitted the experimental data with a linear combination of three independent Gaussian line shapes (Caughey et al., 1981).

NMR Spectroscopy. ^{1}H NMR spectra were recorded using a GE OMEGA 500 spectrometer equipped with a SUN 3 workstation. Hyperfine-shifted NMR spectra were obtained with an 8K data transform of 125 kHz and 7.0 μs 90° pulse by using a conventional WEFT pulse sequence (180−τ−90 acquire) in order to minimize the strong solvent resonances in H_2O solution. A careful setting of the τ value (typically 120−130 ms) can completely eliminate the H_2O signal under rapid repetition of the sequence. We also used a PRESAT pulse sequence with a 1 s presaturation pulse to suppress the residual water resonance. The probe temperature was 23 ± 0.5 °C. The concentration of the sample was about 1 mM in 100 mM sodium phosphate, pD 7.0, and the volume was about 500 μL. Proton shifts were referenced with

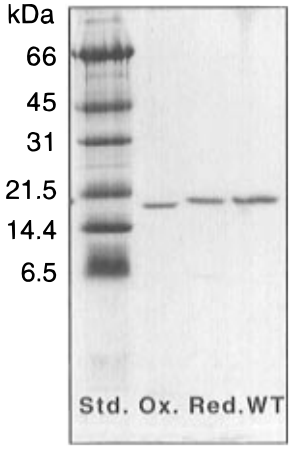

FIGURE 2: SDS−PAGE analysis of the S−S and SH mutants. Std. is the molecular weight standard; WT is wild-type human myoglobin; Ox. is the S−S mutant (oxidized 75C/85C); Red. is the SH mutant (reduced 75C/85C). Each lane contains 0.5 μg of protein.

respect to the signal of the proton resonance of tetramethylsilane (TMS).

RESULTS

Formation and Cleavage of the Disulfide Bond. Figure 2 shows the SDS−polyacrylamide gel electrophoresis (SDS−PAGE) under nonreducing conditions. Since a protein containing an intramolecular disulfide linkage has a smaller radius of gyration and migrates further down the gel (Pollitt & Zalkin, 1983; Perry & Wetzel, 1984), the formation and cleavage of a disulfide bond were detected under these conditions. As illustrated in Figure 2, the S−S mutant (the mutant having the disulfide bond between Cys 75 and Cys 85) migrated faster than wild-type and the SH mutant (the mutant having reduced Cys 75 and Cys 85) myoglobins. We also measured whole molecular weight of the S−S mutant by FAB mass spectroscopy. The molecular weight of the apo S−S mutant was 16 985 ± 0.2 (data not shown). This value is exactly 2 Da smaller than the calculated value of the apo SH mutant, indicating that the two cysteine residues lost two hydrogen atoms by forming the disulfide bond.

Laser Photolysis of Carbonmonoxy Mutants. A set of time courses for CO recombination to the S−S and SH mutant myoglobins at 10 deg intervals (283, 293, and 303 K) are shown in Figure 3. The time axis is plotted on a logarithmic scale. As clearly shown in Figure 3, the time course consists of two distinct phases. The fast phase which is independent of the ligand concentration is the geminate rebinding process, and the second one being dependent on it is the bimolecular rebinding process.

The bimolecular rebinding rate constants (k_{on}) were obtained by millisecond kinetic setup, and the results are listed in Table 1. As shown in Table 1, the k_{on} value for the SH mutant is almost the same as that for wild-type myoglobin, indicating that the effects of replacement of Ile 75 and Glu 85 by cysteine on k_{on} are rather small. However, the rate of CO binding to the S−S mutant (1.8 μM^{-1} s^{-1}) was significantly larger than that of the SH mutant (0.98 μM^{-1} s^{-1}). Temperature dependence of CO bimolecular rebinding for the mutants was measured from 275 to 315 K. The activation energy, E_a, for the bimolecular CO rebinding was estimated by eq 3 as described in Materials and Methods.

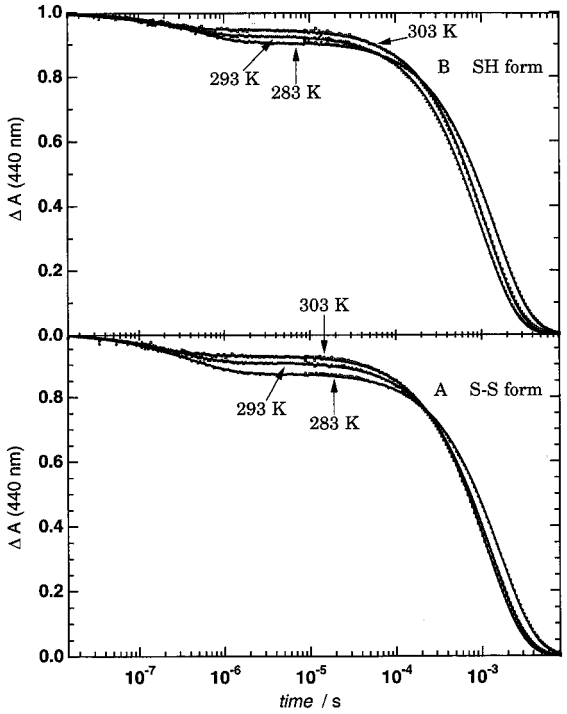

FIGURE 3: Time courses for CO rebinding to the S−S (A) and SH (B) mutants. The dots are the experimental data, and the solid lines are fitting curves simulated by the eq 3. The solid lines are the data, and the dashed lines are fits to two exponential functions.

The activation energy was not affected by the introduction of the disulfide bond.

To gain further insight into this acceleration of bimolecular rebinding rate, we analyzed the rebinding process in more detail. In this work, we adopted the three-state sequential scheme (Alberding et al., 1976; Henry et al., 1983) to the time course of carbon monoxide rebinding (eq 5) and obtained the rate constants for each elementary step. Since the geminate process could be fitted with a single exponential within our experimental error, the model is adequate to our experiments under the present conditions.[3] The parameters for the geminate kinetics are estimated from the data of Figure 3, and the results are summarized in Tables 1 and 2. The rate constant (k_g) for the S−S mutant was virtually the same as that for the SH mutant. On the other hand, the geminate yield for the S−S mutant (0.092 ± 0.001) is significantly larger than that for the SH mutant (0.072 ± 0.001). In the rate constants for the elementary steps, the introduction of the disulfide bond into myoglobin accelerated k_{BA}, the rate for the bond formation from the heme environment to the heme iron (0.27−0.35 s^{-1}), and k_{SB}, the rate for the migration from solvent to the heme environment (14−19 s^{-1}).

Measurement of Dissociation Rate. The time courses of the CO dissociation reaction for the S−S and SH mutants were measured by the conventional NO replacement method

[3] The geminate rebinding for MbCO is distinctly nonexponential and can be fitted more adequately with either a stretched exponential or a biexponential form (Tian et al., 1992). Steinbach (1991) also described this reaction by a time-dependent barrier model, which postured that the barrier to rebinding increases a function of a time as the protein relaxes toward the equilibrium. However, the CO geminate process of human wild-type myoglobin and most mutants under aqueous solution at room temperature can be simulated by a single exponential well (Lambright et al., 1994).

Table 1: Kinetic Parameters for CO Rebinding to Human Myoglobins in 0.1 M Sodium Phosphate Buffer, pH 7.0 at 20 °C

	k_{on} (μM^{-1} s^{-1})	k_{off} (s^{-1})	K_{CO} (μM^{-1})	k_g (μs^{-1})	ϕ_g
S−S	1.8 ± 0.0[a]	0.012 ± 0.001	147 ± 14	3.8 ± 0.1	0.092 ± 0.001
SH SH	0.98 ± 0.01	0.016 ± 0.001	61 ± 4	3.8 ± 0.1	0.072 ± 0.001
wild type	1.1 ± 0.0[a]	0.018 ± 0.001	61 ± 5	3.3 ± 0.1	0.068 ± 0.001

[a] Error is less than 0.03.

Table 2: Kinetic Parameters for CO Rebinding to Human Myoglobins in 0.1 M Sodium Phosphate Buffer, pH 7.0 at 20 °C

	k_{AB} (s^{-1})	k_{BA} (μs^{-1})	k_{BS} (μs^{-1})	k_{SB} (M^{-1} μs^{-1})
S−S	0.013 ± 0.001	0.35 ± 0.01	3.4 ± 0.1	19 ± 0[a]
SH SH	0.017 ± 0.001	0.27 ± 0.01	3.5 ± 0.1	14 ± 0[a]
wild type	0.019 ± 0.001	0.22 ± 0.01	3.1 ± 0.1	16 ± 1

[a] Error is less than 0.5.

Table 3: Activated Parameters for CO Rebinding to Human Myoglobins in 0.1 M Sodium Phosphate, pH 7.0 at 20 °C

	E_a (kJ mol^{-1})	$\Delta V^{\ddagger}$ (cm^3 mol^{-1})
S−S	32 ± 1	−19 ± 0.9
SH SH	33 ± 1	−20 ± 1.2
wild type	36 ± 1	−20 ± 0.4

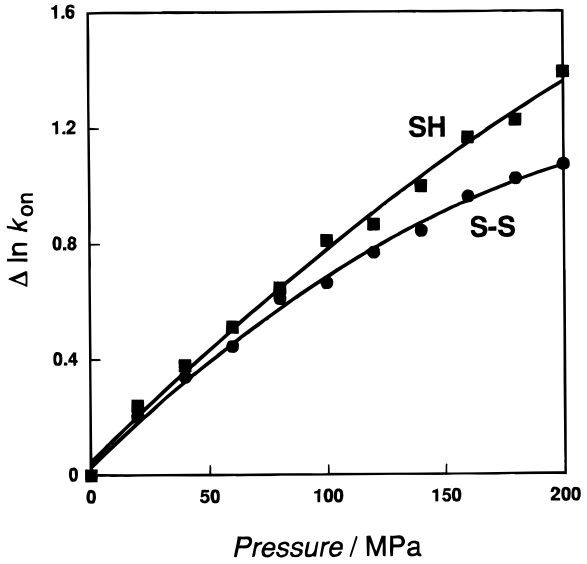

FIGURE 4: Logarithmic plots of the rate constants for the bimolecular CO rebinding reaction vs hydrostatic pressure for the S−S (A) and SH (B) mutants.

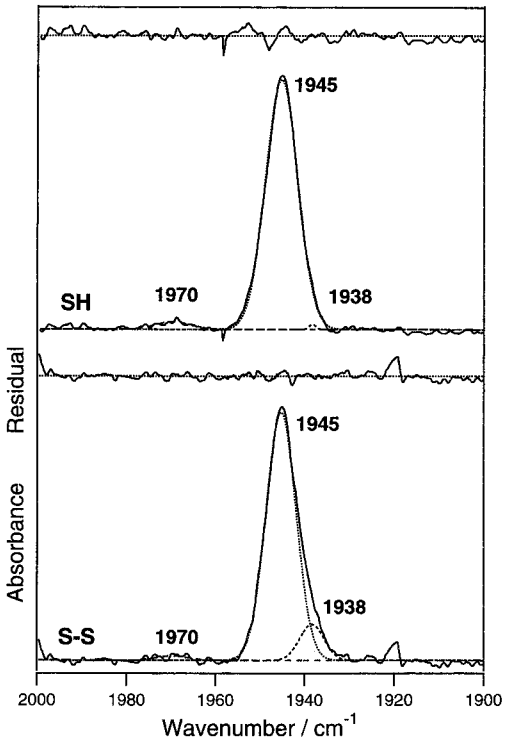

FIGURE 5: FT-IR spectra of the C−O stretching region of the S−S and SH mutant myoglobins. Samples contain 1 mM protein in 0.1 M sodium phosphate buffer at pH 7.0.

(Lambright et al., 1989; Rohlfs et al., 1990), and the values of k_{off} are also summarized in Table 1. Although the k_{off} value for the wild-type myoglobin (0.018 s^{-1}) was a little smaller than that obtained by Dou et al. (0.022 s^{-1}) (1995), the rate constant for the SH mutant (0.016 s^{-1}) was almost identical to that for wild-type myoglobin. As listed in Table 1, the formation of the disulfide bond decelerated the dissociation rate from 0.016 to 0.012 s^{-1}. From the bimolecular rebinding (k_{on}) and dissociation rate (k_{off}) constants, the apparent CO affinity, $K_{CO} = k_{on}/k_{off}$, was estimated as given in Table 1. The S−S mutant shows higher affinity to carbon monoxide (147 μM^{-1}) than the SH mutant (61 μM^{-1}) and wild-type myoglobin (61 μM^{-1}).

Pressure Effect on Bimolecular Ligand Binding. Pressure dependence of the CO bimolecular rebinding kinetics of the S−S and SH mutants is given in Figure 4, and their activation volumes, $\Delta V^{\ddagger}$, are listed in Table 3. The time courses at the elevated pressure we applied here were fitted by a simple single exponential within experimental error (results not shown). The rates of CO rebinding for both mutant myoglobins were accelerated, and the apparent quantum yields were decreased by pressurization as found for native myoglobin (Adachi & Morishima, 1989). The activation volume of CO rebinding in the S−S mutant was identical to that in the SH mutant. In the pressure dependence of the rebinding rate for the S−S mutants, however, some deviations from that for the SH mutant were observed at the elevated pressure.

Infrared Spectra of Carbonmonoxy Mutant and Wild-Type Myoglobins. The infrared spectra for carbonmonoxy S−S and SH mutant myoglobins in the region from 2000 to 1900 cm^{-1} at pH 7.0 are shown in Figure 5. All spectra could be decomposed by the sum of three Gaussian functions. The positions of the IR stretching band and population of conformers for wild-type and mutant myoglobins are summarized in the Table 4. In myoglobin, at least three different CO conformers can be identified in IR spectra under various conditions and designated as listed in Table 4 (Caughey et al., 1969,1981; Makinen et al., 1979; Ansari et al., 1987; Frauenfelder et al., 1988). For human wild type myoglobin, the main C−O stretch mode (A_1) was observed at 1945 cm^{-1}, and one minor band appeared at 1967 (A_0) cm^{-1} at room temperature. On the other hand, both of the mutants exhibited three C−O stretching bands: one major band at

Table 4: IR Stretching Band and Population of Conformers for Wild-Type and Mutant Myoglobins

	A_0, cm^{-1} (%)	A_1, cm^{-1} (%)	A_3, cm^{-1} (%)
wild type	1967 (3)	1945 (97)	—[a]
S−S	1970 (2)	1945 (86)	1938 (12)
SH	1970 (3)	1945 (95)	1938 (2)

[a] Not detected.

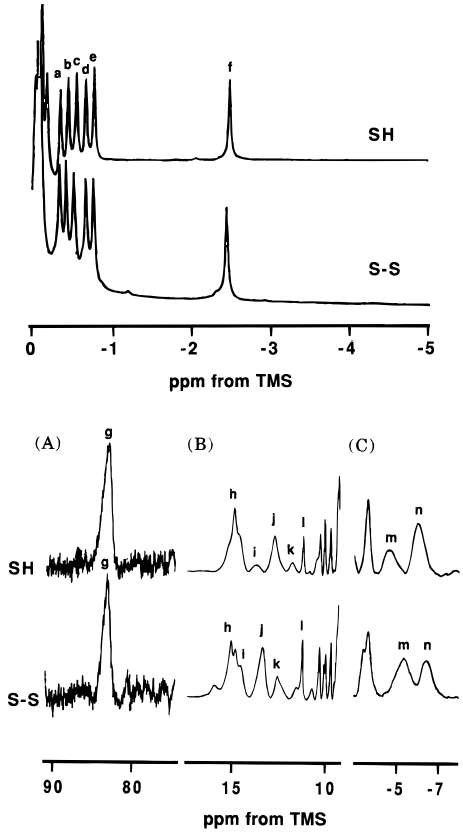

FIGURE 6: ^{1}H NMR spectra of the S−S and SH mutants. The samples contain 1 mM protein in 0.1 M sodium phosphate buffer at pD 7.0: (A) carbonmonoxy form; (B) deoxy form.

1945 (A_1) cm^{-1} and two minor bands at 1970 (A_0) and 1938 (A_3) cm^{-1}. Although the peak positions of both mutants were identical, the population of the A_3 conformer increased from 2% to 12% by the disulfide bond formation. The bandwidth of the main conformer for the S−S mutant was 8.5 cm^{-1}, which is also almost identical to that for the SH mutant (8.8 cm^{-1}) and wild-type myoglobin (9.0 cm^{-1}).

NMR Spectra of Mutant and Wild-Type Myoglobins. In Figure 6, the ^{1}H NMR spectra of carbonmonoxy mutant myoglobins are illustrated. The ring-current-shifted proton peak at −2.5 ppm (f) in Figure 6A, which has been assigned to a methyl group of Val 68, serves as a marker for the structure of the heme vicinity in carbonmonoxymyoglobin (Shulman et al., 1970). The resonance position of this methyl group in the mutants was identical with that of wild-type myoglobin. The signals observed in the upfield region (a−e), which are assignable to a methyl group of Val 17, Leu 29, and Val 68 (Shulman et al., 1970; Dalvit & Wright, 1987) as listed in Table 5, were also insensitive to the formation of the disulfide bond, although slight shifts were detected in their signal positions.

The NMR spectra of the deoxygenated form of the S−S and SH mutants are shown in Figure 6B. In a far-downfield region (A), one exchangeable proton peak was observed (g). This resonance was assigned to the $N_\delta H$ proton of the proximal histidine (Goff & La Mar, 1977; La Mar et al., 1977, 1993). The signal for wild-type myoglobin is observed at 78.5 ppm from TMS, whereas the S−S mutant bears the signal at 83.2 ppm, which is identical to that for the SH mutant. The resonance of the 5-methyl group at the heme (h) appeared at 15.1 ppm for the S−S mutant and 14.9 ppm for the SH mutant as shown in (B). The peak at 11.2 ppm in the S−S mutant (k) is assignable to the 3-methyl group, which was also observed at the same position for the SH mutant. However, in the region (B), the resonances i and j, which were assigned to 6-H_α, 4-H_α of the heme, respectively, shifted to downfield, and significant spectral changes in the upfield (C) were detected. The SH mutant exhibited the resonances from γ-methyl groups of Val 68 at −4.7 (m) and −6.0 ppm (n), whereas the corresponding signals for the S−S mutant were −5.3 (m) and −6.4 ppm (n). These NMR spectral changes indicate that some conformational changes are induced by the formation of the disulfide bond at the EF corner in the unliganded form. The prominent NMR resonances are listed in Table 6.

Table 5: Proton NMR Chemical Shifts of Mutant Carbomonoxymyoglobins in Sodium Phosphate, pD 7.0 at 23 °C (ppm from TMS)

	Val 17 $C_\gamma H_3$ a	Leu 29 $C_\delta H_3$ b	Val 17 $C_\gamma H_3$ c	Val 68 $C_\gamma H_3$ d	Leu 29 $C_\delta H_3$ e	Val 68 $C_\gamma H_3$ f
S−S	−0.36	−0.46	−0.56	−0.68	−0.78	−2.5
SH SH	−0.35	−0.43	−0.53	−0.68	−0.77	−2.5
wild type	−0.35	−0.43	−0.56	−0.60	−0.79	−2.5

Table 6: Proton NMR Chemical Shifts of Mutant Deoxymyoglobins in Sodium Phosphate, pH 7.0 at 23 °C (ppm from TMS)

	His 93	heme				Ile 107	Val 68	
	$N_\delta H$ g	5-CH_3 h	6-H_α i	4-H_α j	3-CH_3 k	$C\gamma H_3$ l	$C_\gamma H_3$ m	$C_\gamma H_3$ n
S−S	83.2	15.1	14.5	13.4	11.2	11.8	−5.3	−6.4
SH SH	83.2	14.9	13.7	12.6	11.2	12.6	−4.7	−6.0
wild type[a]	78.5	14.8	14.1	13.0	10.8	13.0	−4.5	−7.3

[a] Assignments of wild-type horse myoglobin are given in Busse and Jue (1994).

Near-Infrared Absorption Spectra of Deoxymyoglobins. The near-infrared absorption spectra (band III) for the S−S and SH mutant myoglobins in the deoxy form are illustrated in Figure 7. These spectra can be well described by a Gaussian function on top of a cubic polynomial background and the center frequency for the SH mutant was 762.4 nm, corresponding to that for wild-type myoglobin. The wavelength of the S−S mutant was 763.8 nm, which showed a 1.4 nm red shift from that of the SH mutant. Since this band arises from electron transfer from the a_{2u} orbital of the porphyrin to the d_{yz} orbital of heme iron (Eaton & Hofrichter, 1981), the red shift in the S−S mutant is interpreted as a decrease in the transition energy between the two orbitals (Sassaroli & Rousseau, 1987; Campbell et al., 1987), and it can be concluded that displacement of the heme iron from the heme plane in the S−S mutant was smaller than that of the SH mutant.

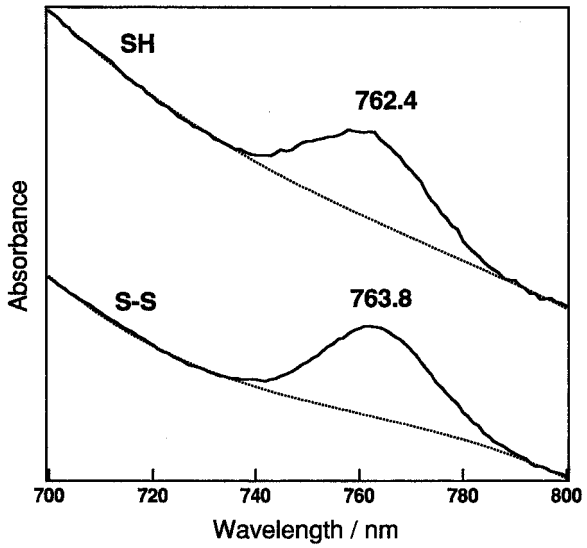

FIGURE 7: Near-infrared absorption spectra of the deoxy mutant myoglobins. The data were modeled with a Gaussian function plus a cubic polynomial function. The dashed lines represent the background. Samples contain 1 mM protein in 0.1 M sodium phosphate buffer at pH 7.0.

DISCUSSION

Effects of the Disulfide Bond on the Heme Environmental Structure. The IR spectra of carbonmonoxy complexes of heme proteins have provided unique information on the local environment of the distal side of the heme pocket (Balasubramanian et al., 1993; Li et al., 1994; Decature & Boxer, 1995). Recently, the electrostatic potential around the iron-bound carbon monoxide is considered to be one of the major factors for the C−O stretching frequencies (Li & Spiro, 1988; Park et al., 1991; Ray et al., 1994; Li et al., 1994). It has been revealed that the downshift of the C−O stretching mode is induced by the presence of positive charges, whereas the presence of negative charges causes the upshift of the mode (Li & Spiro, 1988; Oldfield et al., 1991; Park et al., 1991; Ray et al., 1994; Li et al., 1994). As shown in Figure 5 and Table 4, the peak positions for the S−S mutant are identical to those for the SH mutant. With formation of the disulfide bond, however, the A_3 conformer increased from 2% to 12%. The A_3 conformer was observed for sperm whale myoglobin with 30% content, while this conformer was not detected for the human wild-type myoglobin (Adachi et al., 1992; Balasubramanian et al., 1993), even though the two myoglobins have similar heme environmental structures. Increase in A_3 conformer by the disulfide bond formation may suggest the induction of some structural changes of heme pocket residues. However, since the IR-detected population change is very sensitive to the environment around ligated carbon monoxide, this disulfide bond-induced change would be much smaller than those observed for the distal pocket mutants (Adachi et al., 1992; Balasubramanian et al., 1993; Li et al., 1994).

In ^{1}H NMR spectra of the carbonmonoxy form of the mutants, the peaks of γ-methyl groups of Val 68 in the S−S form appeared at −0.68 (d) and −2.5 ppm (f) from TMS, which are almost identical with those of the SH form. The peak positions of δ-methyl groups of Leu 29 and γ-methyl groups of Val 17 in the S−S form were also in good agreement with those of the SH form. Since the ring current shifts are sensitive to conformational alteration near the porphyrin ring (Shulman et al., 1970), the structural changes induced by the S−S bond formation would be small in the heme environment of the carbonmonoxy form.

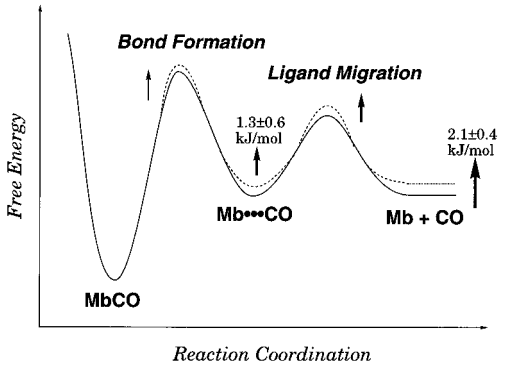

FIGURE 8: Relative free energy schematically plotted vs the reaction coordinate. The solid and dashed curves represent the free energies for the SH and S−S myoglobins, respectively.

In the deoxygenated state, however, some significant structural differences between the S−S and SH mutants were observed. In Figure 6B, the signal patterns in (B) and (C) for the S−S mutant are significantly different from those of the SH mutant, although the signal position of $N_\delta H$ in the proximal histidine (g) is identical. Since the resonances m and n have been assigned to γ-methyl groups of Val 68, which is located in the distal side, formation of the disulfide bond induced some structural changes in the distal side. The peak position of the charge transfer band (band III) in the near-IR region (Figure 7) also shows the red shift for the S−S mutant. The red shift suggests that displacement of the heme iron is decreased in the deoxygenated S−S mutant.

These preferential structural changes in the deoxygenated form of the S−S mutant can be deduced from the structural differences around the EF corner between the deoxy and carbonmonoxy forms. The crystallographic structure of native myoglobin has revealed that the distance from the γ-methylene carbon of Ile 75 to the γ-carbonyl carbon of Glu 85 is 4.05 Å in the carbonmonoxy form (Cheng & Schoenborn, 1991), whereas, in the deoxygenated form, the distance becomes longer (4.78 Å) (Takano, 1977). Since the typical bond length of a disulfide bond is about 2 Å, the conformational strains in the EF corner should be enhanced in the deoxygenated S−S mutant than those in the carbonmonoxy form.

Ligand Binding Properties. On the basis of the present kinetic results, the free energy diagrams for the binding of CO to the S−S and SH mutants are schematically shown in Figure 8, where the free energy of the system is depicted as a function of the reaction coordinate. The increased affinity of carbon monoxide (K_{CO}) for the S−S mutant corresponds to the increased free energy difference between the states "MbCO" and "Mb + CO" in Figure 8. More prominent conformational changes in the deoxygenated form imply that the difference of the free energy can be localized in the deoxygenated form, which is represented as Mb + CO in the figure. The energy level of the state MbCO for the S−S mutant would be the same as that for the SH mutant. Taking into account that the dissociation rate (k_{AB}) was slowed down and the bond formation (k_{BA}) was accelerated, the energy level of the state "Mb···CO" and the energy barrier for the bond formation would be raised as shown in the figure. Since previous studies (Carver et al., 1990; Gibson et al., 1992)

reported that the bond formation process is affected by the local fluctuations immediate near the ligand of the heme, which would be determined by the motions of the side chains of the amino acid residues in the distal side, the elevated energy barrier for the bond formation process can be induced by the restricted motion at the EF corner.

On the other hand, the ligand migration rate was accelerated (k_{SB}), while the rate of ligand diffusion from the interior of protein to solvent (k_{BS}) was not changed. These alterations in the migration process indicate that the energy barrier for the ligand migration becomes higher by formation of the disulfide bond. Since the protein fluctuations play key roles in forming the "ligand entry channel" to pass through the interior of the protein (Takano, 1977; Phillips, 1980; Kuriyan et al., 1986; Elber & Karplus, 1990), it can be considered that the perturbation in the motion of the EF corner is one of the factors for the enhancement of the energy barrier in the ligand migration process.

The free energy changes for the ligand binding were also encountered in the distal histidine and leucine-29 mutant myoglobins (Springer et al., 1994). By the substitution of these residues, drastic changes were induced in heme environmental structure (Quillin et al., 1993). The hydrogen bond of the distal histidine was disrupted in the mutant myoglobin having the mutation at the distal histidine, which leads to an increase in the ligand association rates (Carver et al., 1990; Quillin et al., 1993). The mutation at leucine-29 (B10) remarkably reduced the ligand binding rate probably due to introducing extra water molecules into the heme pocket (Rohlfs et al., 1990; Carver et al., 1990; Adachi et al., 1992). Most of the distal histidine mutants exhibited 10−15-fold larger binding rates (k_{on}). In other words, the energy change between the deoxy and carbonmonoxy forms was up to 7 kJ/mol. Present results showed that formation of the disulfide bond at the EF corner only affected about 2 kJ/mol in the free energy difference between the two states. The effects of the disulfide bond formation on the binding rate and free energy for the ligand binding were somewhat smaller than those of the substitution of the distal amino acid residues.

Effects of Disulfide Bond Formation on Fluctuation. In spite of the EF corner being near the active site for the ligand binding, functional and structural deviations of the S−S mutant from the SH mutant were smaller than we expected. It is rather likely that the effects of the disulfide bond on protein fluctuation are localized at the mutated site as found for the lysozyme C77A/C95A mutant (Kidera et al., 1994). In the lysozyme mutant, although the effects of the mutation on the internal fluctuations were detected in the long flexible loop region containing residue 77, the other mutation site 95 in the α-helix did not exhibit any changes in the dynamic structure. They concluded that the cleavage of the disulfide linkage in the mutant lysozyme caused no significant changes in the protein fluctuations except for the mutated site. Schulman and Kim (1994) also reported that amide proton exchange rates in BPTI (bovine pancreatic trypsin inhibitor) mutants, in which disulfide bonds are removed, were very similar to that of wild-type BPTI and the structural changes were localized at the mutated amino acid residues.

In summary, the present results indicate that the restriction effects by formation of the disulfide bond at the EF corner on protein fluctuation may be localized in the mutation site and the disulfide linkage cannot seriously affect the dynamic properties of the E- and F-helices nor the ligand binding process. Our preliminary results from the SDS denaturation studies also showed that the free energy for the denaturation was almost insensitive to the disulfide bond formation. The other regions and motions would be crucial for regulating the fluctuation in the ligand binding. Some mutants having other disulfide bonds or cross linkages at the various positions are now being investigated in our group.

ACKNOWLEDGMENT

We are grateful to Prof. S. G. Boxer and Dr. R. Varadarajan (Stanford University) for a gift of the expression vector of the human myoglobin gene. We are also grateful to Dr. T. Iizuka, Dr. Y. Shiro, and Dr. S. Adachi [The Institute of Physical and Chemical Research (RIKEN)] for the nanosecond laser photolysis measurement and for valuable discussions. We are obliged to Prof. Y. Watanabe (Institute of Molecular Science) for his fruitful discussion. We thank Dr. Y. Wada (Osaka Medical Center and Research Institute for Maternal and Child Health) for the FAB mass spectral measurement.

REFERENCES

Adachi, S., & Morishima, I. (1989) *J. Biol. Chem. 264*, 18896−18901.

Adachi, S., Sunohara, N., Ishimori, K., & Morishima, I. (1992) *J. Biol. Chem. 267*, 12614−12621.

Alberding, N., Chan, S. S., Eisenstein, L., Frauenfelder, H., Good, D., Gunsalus, I. C., Nordlung, T. M., Perutz, M. F., Reynolds, A. H., & Sorensen, L. B. (1978) *Biochemistry 17*, 43−51.

Ansari, A., Berendzen, J., Braunstein, D., Cowen, B. R., Frauenfelder, H., Hong, M. K., Iben, I. E. T., Johnson, E. T., Ormos, P., Sauke, T. B., Scholl, R., Schulte, A., Steinbach, P. J., Vittitow, P. J., & Young, R. D. (1987) *Biophys. Chem. 26*, 337−355.

Antonini, E., & Brunori, M. (1971) *Hemoglobin and Myoglobin in Their Reactions with Ligands*, North-Holland, Amsterdam.

Austin, R. H., Beeson, K. W., Eisenstein, L., Frauenfelder, H., & Gunsalus, I. C. (1975) *Biochemistry 14*, 5355−5373.

Balasubramanian, S., Lambright, D. G., Marden, M. C., & Boxer, S. G. (1993) *Biochemistry 32*, 2202−2212.

Busse, S. C., & Jue, T. (1994) *Biochemistry 33*, 10934−10943.

Campbell, B. F., Chance, M. R., & Friedman, J. M. (1987) *Science 238*, 373−376.

Careaga, C. L., & Falke, J. J. (1992) *Biophys. J. 62*, 209−219.

Carver, T. E., Rohlfs, R. J., Olson, J. S., Gibson, Q. H., Blackmore, R. S., Springer, B. A., & Sligar, S. G. (1990) *J. Biol. Chem. 265*, 20007−20020.

Caughey, W. S., Alben, J. O., McCoy, S., Boyer, S. H., Carache, S., & Hathaway, P. (1969) *Biochemistry 8*, 59−62.

Caughey, W. S., Shimada, H., Choc, M. G., & Tucker, M. P. (1981) *Proc. Natl. Acad. Sci. U.S.A. 75*, 2903−2907.

Chatfield, M. D., Walda, K. N., & Madge, D. (1990) *J. Am. Chem. Soc. 112*, 4680−4687.

Cheng, X., & Schoenborn, B. P. (1991) *J. Mol. Biol. 220*, 381−399.

Daggett, V., & Levitt, M. (1993) *J. Mol. Biol. 232*, 600−619.

Dalvit, C., & Wright, P. E. (1987) *J. Mol. Biol. 194*, 313−327.

Decatur, S. M., & Boxer, S. G. (1995) *Biochem. Biophys. Res. Commun. 212*, 159−164.

Dou, Y., Admiraal, S. J., Ikeda-Saito, M., Krzywda, S., Wilkinson, A. J., Li, T. S., Olson, J. S., Prince, R. C., Pickering, I. J., & George, G. N. (1995) *J. Biol. Chem. 270*, 15993−16001.

Eaton, W. A., & Hofrichter, J. (1981) *Methods Enzymol. 76*, 175−261.

Elber, R., & Karplus, M. (1990) *J. Am. Chem. Soc. 112*, 9161−9175.

Frauenfelder, H., Petsko, G. A., & Tsernoglou, D. (1979) *Nature 280*, 558−563.

Frauenfelder, H., Park, K. D., & Young, R. D. (1988) *Annu. Rev. Biophys. Chem. 17*, 451−479.
Frauenfelder, H., Sligar, S. G., & Wolynes, P. G. (1991) *Science 254*, 1598−1603.
Gibson, Q. H., Olson, J. S., McKinnie, R. E., & Rohlfs, R. J. (1986) *J. Biol. Chem. 261*, 10228−10239.
Gibson, Q. H., Regan, R. R., Elber, R., Olson, J. S., & Carver, T. E. (1992) *J. Biol. Chem. 267*, 22022−22034.
Goff, H. M., & La Mar, G. N. (1977) *J. Am. Chem. Soc. 99*, 6599−6606.
Gurd, F. R. N., & Rothgeb, T. M. (1979) *Adv. Protein Chem. 33*, 73−165.
Gusev, N. B., Grabarek, Z., & Gergely, J. (1991) *J. Biol. Chem. 266*, 16622−16626.
Henry, E. R., Sommer, J. H., Hofrichter, J., & Eaton, W. A. (1983) *J. Mol. Biol. 166*, 443−451.
Jeng, M.-F., & Dyson, H. J. (1995) *Biochemistry 34*, 611−619.
Kanaya, S., Katsuda, C., Kimura, S., Nakai, T., Kitakuni, E., Nakamura, H., Katayanagi, K., Morikawa, K., & Ikehara, M. (1991) *J. Biol. Chem. 266*, 6038−6044.
Karplus, M., & McCammon, J. A. (1983) *Annu. Rev. Biochem. 52*, 263−300.
Kidera, A., Inaka, K., Matsushima, M., & Go, N. (1994) *Protein Sci. 3*, 92−102.
Kunkel, T. A. (1985) *Proc. Natl. Acad. Sci. U.S.A. 82*, 488−492.
Kuriyan, J., Wilz, S., Karplus, M., & Petsko, D. A. (1986) *J. Mol. Biol 192*, 133−154.
La Mar, G. N., Budd, D. L., & Goff, H. M. (1977) *Biochem. Biophys. Res. Commun. 77*, 104−110.
La Mar, G. N., Davis, N. L., Johnson, R. D., Smith, W. S., Hauksson, J. B., Budd, D. L., Dalichow, F., Langry, K. C., Morris, I. K., & Smith, K. M. (1993) *J. Am. Chem. Soc. 115*, 3869−3876.
Lambright, D. G., Balasubramanian, S., & Boxer, S. G. (1989) *J. Mol. Biol. 207*, 289−299.
Lambright, D. G., Balasubramanian, S., & Boxer, S. G. (1991) *Chem. Phys. 158*, 249−260.
Lambright, D. G., Balasubramanian, S., Decatur, S. M., & Boxer, S. G. (1994) *Biochemistry 33*, 5518−5525.
Li, T., Quillin, M. L., Phillips, G. N., Jr., & Olson, J. S. (1994) *Biochemistry 33*, 1433−1446.
Li, X.-Y., & Spiro, T. G. (1988) *J. Am. Chem. Soc. 110*, 6024−2033.
Makinen, M. W., Houtchens, R. A., & Caughey, W. S. (1979) *Proc. Natl. Acad. Sci. U.S.A. 76*, 6042−6046.
Matsumura, M., Becktel, W. J., Levitt, M., & Matthews, B. W. (1989) *Proc. Natl. Acad. Sci. U.S.A. 86*, 6562−6566.
Newmann, R. C., Jr., Kauzmann, W., & Zipp, A. (1973) *J. Phys. Chem. 77*, 2687−2691.
Oldfield, E., Guo, K., Augspurger, J. D., & Dykstra, C. E. (1991) *J. Am. Chem. Soc. 113*, 7537−7541.
Olson, J. S., Mathews, A. J., Rohlfs, R. J., Springer, B. A., Egeberg, K. D., Sligar, S. G., Tame, J., Renaud, J.-P., & Nagai, K. (1988) *Nature 336*, 265−266.
Pantoliano, M. W., Landner, R. C., Bryan, P. N., Rollence, M. L., Wood, J. F., & Poulos, T. L. (1987) *Biochemistry 26*, 2077−2082.
Park, K. D., Guo, K., Adeboun, F., Chiu, M. L., Sligar, S. G., & Oldfield, E. (1991) *Biochemistry 30*, 2333−2347.
Perry, L. J., & Wetzel, R. (1984) *Science 226*, 555−557.
Perutz, M. F. (1965) *J. Mol. Biol. 13*, 646−668.
Phillips, D. C. (1966) *Sci. Am. 215*, 75−80.
Phillips, S. E. V. (1980) *J. Mol. Biol. 142*, 531−554.
Pollitt, S., & Zalkin, H. (1983) *J. Bacteriol. 153*, 27−32.
Powers, L., Chance, B., Campbell, B., Friedman, J., Khalid, S., Kumar, C., Naqui, A., Reddy, K. S., & Zhou, Y. (1987) *Biochemistry 26*, 4785−4796.
Quillin, M. L., Arduini, R. M., Olson, J. S., & Phillips, G. N., Jr. (1993) *J. Mol. Biol. 234*, 140−155.
Ray, G. B., Li, X.-Y., Ibers, J. A., Sessler, J. L., & Spiro, T. G. (1994) *J. Am. Chem. Soc. 116*, 162−176.
Rohlfs, R. J., Mathews, A. J., Carver, T. E., Olson, J. S., Springer, B. A., Egeberg, K. D., & Sligar, S. G. (1990) *J. Biol. Chem. 265*, 3168−3176.
Sassaroli, M., & Rousseau, D. L. (1987) *Biochemistry 26*, 3092−3098.
Schulman, B. A., & Kim, P. S. (1994) *Protein Sci. 3*, 2226−2232.
Shulman, R. G., Wüthrich, K., Yamane, T., Patel, D. J., & Blumberg, W. E. (1970) *J. Mol. Biol. 53*, 143−157.
Springer, B. A., Sligar, S. G., Olson, J. S., & Phillips, G. N., Jr. (1994) *Chem. Rev. 94*, 699−714.
Steinbach, P. J., Ansari, A., Berendzen, J., Braunstein, D., Chu, K., Cowen, B. R., Ehrenstein, D., Frauenfelder, H., Johnson, J. B., Lamb, D. C., Luck, S., Mourant, J. R., Nienhaus, G. U., Ormos, P., Philipp, R., Xie, A., & Young, R. D. (1991) *Biochemistry 30*, 3988−4001.
Takano, T. (1977) *J. Mol. Biol. 110*, 537−584.
Tian, W. D., Sage, J. T., Srajer, V., & Champion, P. M. (1992) *Phys. Rev. Lett. 68*, 408−411.
Tian, W. D., Sage, J. T., Champion, P. M., Chien, E., & Sligar, S. G. (1996) *Biochemistry 35*, 3487−3502.
Unno, M., Ishimori, K., & Morishima, I. (1990) *Biochemistry 29*, 10199−10205.
Unno, M., Ishimori, K., & Morishima, I. (1991) *Biochemistry 30*, 10679−10685.
Unno, M., Ishimori, K., Ishimura, Y., & Morishima, I. (1994) *Biochemistry 33*, 9762−9768.
Varadarajan, R., Szabo, A., & Boxer, S. G. (1985) *Proc. Natl. Acad. Sci. U.S.A. 82*, 5681−5684.
Varadarajan, R., Lambright, D. G., & Boxer, S. G. (1989) *Biochemistry 28*, 3771−3781.

BI960591Z